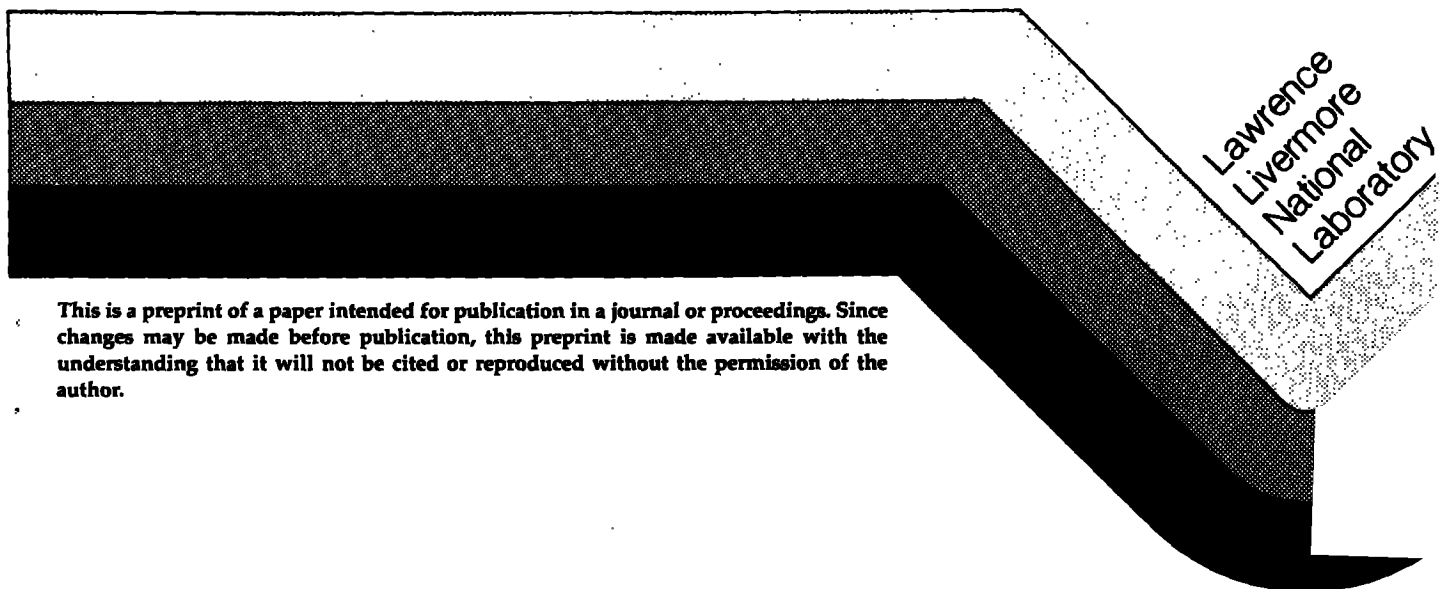# NON-ISOTHERMAL FEM ANALYSES OF

LARGE-STRAIN BACK EXTRUSION FORGING

E. C. Flower
J. O. Hallquist
A. B. Shapiro

CIRCULATION C
SUBJECT TO RECA
IN TWO WEEKS

June 19, 1986

DISCLAIMER

NON-ISOTHERMAL FEM ANALYSES OF LARGE-STRAIN BACK EXTRUSION FORGING

ABSTRACT

Back extrusion forging is a complex metal forming operation dominated by large-strain, non-isothermal deformation. NIKE2D, a fully vectorized implicit finite-element program developed at Lawrence Livermore National Laboratory, was applied to a two-stage isothermal back extrusion forging process. Modeling of the forging process required special features in the FEM code such as friction and interactive rezoning that allows for remeshing of the distorted mesh while maintaining a complete history of all the state variables. To model conditions of the non-isothermal forging process required implementing TOPAZ2D, our LLNL-developed two-dimensional implicit finite element code for heat conduction analysis, as a subroutine into NIKE2D. The fully coupled version maintains all the original features of both codes and can account for the contribution of heat generation during plastic deformation. NIKE/TOPAZ-2D was applied to the piercing operation of the back extrusion forging process. The thermal deformation history of the die, punch, and workpiece and the effective plastic strains were calculated.

Computer modeling of metal forming processes is an extension of an ongoing effort at Lawrence Livermore National Laboratory to expand the application of our finite-element method (FEM) codes to the manufacturing process. Dependability and performance of a design, as well as rapid design-to-fabrication, have always had a high priority at LLNL. These criteria have driven the development of sophisticated FEM codes that aid in early evaluation of a proposed design. In addition to reliability and performance of a design, LLNL has the responsibility of the design through manufacture and is concerned with the integrity and fabricablity of the components. In the early stages of design, there is often the need to consider the actual manufacturing process of a proposed component, since a sound conceptual design can end up as a failure because of problems encountered in the fabricating process.

Computer modeling of metal-forming processes requires knowledge of the boundary conditions of the fabrication process and the material behavior. Qualitative physical concepts have to be transformed into quantitataive numerical descriptions. In metal-forming analysis, the FEM code has to simulate the evolution of stresses, strains, temperatures, and other state variables as a metal body deforms, and model to appropriate accuracy the physical conditions surrounding the deforming metal. For example, friction between the die and workpiece, an important physical consideration in metal forming, must be treated in the modeling of the die-workpiece interface. We also know that most metal-forming operations involve large plastic strains that distort the FEM mesh as the deformation proceeds. Severe distortion of

the mesh can cause the numerical solution to lose accuracy or, even worse, to numerically diverge and terminate without completing the forming process. For proper consideration of large deformations, the FEM code must have the ability to "rezone" i.e., smooth the distorted mesh without losing the deformation history. In addition, several classes of metal forming are non-isothermal and require calculating, the effects of heat transfer and heat generation during the deformation process. These are just some of the features required in a computer code to model metal forming with sufficient accuracy.

NIKE2D,[1] a large-deformation, implicit, elastic/plastic FEM code developed at LLNL, has proven highly reliable for computational analysis in support of many laboratory programs. NIKE2D contains many features that are required for forming analysis:

- Elastic/plastic/thermal creep material models

- Large-scale, non-linear deformation

- Axisymmetric, plane strain, and plane stress analysis capability

- Interface treatment of friction

- Load history, including interface pressures and die stresses

- Rezoning

NIKE2D has been applied to several metal forming problems.[2] Its demonstrated success has encouraged further development to address a larger variety of forming processes. This includes the implementation of consitutive models such as a rate dependent plasticity which is required to analyze the superplastic forming process and non-isothermal forging. Other developments in NIKE2D such as the implementation of several iteration schemes, provides the analyst a choice of convergence method to solve a problem. For example, the arc length or Rik's method allows solutions to be obtained in forming problems such as hydrostatic forward extrusion where loading instabilities occur from the pressure on the billet varying as the material extrudes through the die. When unstable loading occurs, normal iterative techniques fail to converge and the calculation is terminated without obtaining a solution.

At LLNL, NIKE2D is undergoing continual development to improve its capabilities, computational efficiency, and accuracy. NIKE2D has been applied to metal forming processes including:

Rolling

Machining

Upset forging

Closed-die Forging

Forward hydrostatic extrusion

Back extrusion

Sheet forming

Superplastic forming

Hydroforming

TOPAZ2D[3] is a general purpose two-dimensional finite element code for nonlinear heat transfer analysis. Material properties may be temperature dependent and either isotropic or orthotropic. A variety of time and temperature dependent boundary conditions can be specified including temperature, flux, convection and radiation. An implicit time integration formulation is used for transient problems. In a nonlinear problem, functional iteration with under relaxation is used to satisy energy conservation at each time step.

As in NIKE2D, generality, computation efficiency and accuracy are important considerations in the TOPAZ2D code. TOPAZ2D has been applied successfully to the analysis of arc welding[4] and heat treatment of components,[5] and has potential for studying casting and quenching problems.

NIKE2D and TOPAZ2D are supported by the LLNL-developed interactive pre-processor MAZE,[6] a general-purpose mesh generator that creates the complete NIKE2D/TOPAZ2D input file, and by an interactive post-processor, ORION,[7] that allows for graphic representation of the computational results. ORION reads the binary plot files generated by NIKE2D and TOPAZ2D and plots contours, time histories, deformed shapes and temperature. ORION can also compute a variety of strain measures, interface pressures along slide-lines, reaction forces along constrained boundaries, and momentum.

The full coupling of NIKE2D and TOPAZ2D have provided a new capability to perform realistic numerical simulation of non-isothermal metal forming problems. The following briefly outlines the approach.

The linear momentum and energy balance laws are:

$$\nabla \cdot \sigma + b = \rho \, a$$

$$\sigma \cdot \nabla v - \nabla \cdot g + r = \dot{E}. \tag{1}$$

where v is the particle velocity $\dot{x}$, a the particle acceleration $\dot{v}$, σ is the Cauchy stress tensor, g the heat flux vector per current area, ρ the current density, E the internal energy and $\nabla \cdot$ is the divergence operator per current configuration x. ∇v is the velocity gradient, b the body force, and r the internal heat generation. The time derivates are material, and thus simple partials for a Lagrangian frame where coordinates are assigned to material points.

The heat flux vector g for conduction of heat in an anisotropic solid is

$$g = - K \, \nabla \, \theta \tag{2}$$

where K is the thermal conductivity tensor and θ is the temperature. The energy balance, Eq. (1), is then expressed as

$$\sigma \cdot \nabla v + \nabla \cdot K \, \nabla \theta + r = \dot{E} \tag{3}$$

subject to the mixed boundary condition

$$- K \, \nabla \theta \cdot n = \alpha \, \theta - \beta \tag{4}$$

This boundary condition can represent surface heat flux, convection, or radiation depending on the definition of α and β.

The energy and momentum equations with energy dependent mechanical material models must be solved simultaneously in a fully coupled thermo-mechanical code. To achieve this, we use operator splitting. the energy balance is solved including the heat due to the stress power term. The updated temperatures are then used in the constitutive evaluation as we solve the momentum balance. We iterate for convergence and then proceed to the next step. In most forming calculations, we may neglect $\rho \underset{\sim}{a}$ in (1a) due to the quasi-static nature of the process.

For path dependent plasticity we assume that

$$\dot{\underset{\sim}{\sigma}} = \dot{\underset{\sim}{\sigma}} (\underset{\sim}{\sigma}, \nabla \underset{\sim}{v}, E) \tag{5}$$

and update the stresses incrementally

$$\underset{\sim}{\sigma}^{n+1/2} = \underset{\sim}{\sigma}^{n} + \dot{\underset{\sim}{\sigma}}^{n+1/2} \Delta t \tag{6}$$

We use the Green-Naghdi rate

$$\overset{\triangledown}{\underset{\sim}{\sigma}} = \dot{\underset{\sim}{\sigma}} + \underset{\sim}{\sigma}\underset{\sim}{\Omega} - \underset{\sim}{\Omega}\underset{\sim}{\sigma} = \underset{\sim}{C} \dot{\underset{\sim}{\varepsilon}} \tag{7}$$

where, $\underset{\sim}{C}$ is the constitutive matrix, $\dot{\underset{\sim}{\varepsilon}}$ is the strain rates and

$$\underset{\sim}{\Omega} = \dot{\underset{\sim}{R}} \underset{\sim}{R}^{t} \tag{8}$$

where $\underset{\sim}{R}$ is found by applying the polar decomposition theorem to the deformation gradient matrix $\underset{\sim}{F}$, i.e.,

$$\underset{\sim}{F} = \underset{\sim}{R} \, \underset{\sim}{U} \tag{9}$$

Plasticity in our material models is treated by using a radial return algorithm that is not only accurate but computationally efficient. Presently, there are eleven materials including thermo-elastic-plastic-creep and unified creep plasticity.

The following example illustrates the capability of the NIKE/TOPAZ software to address metal forming problems. In particular this example, we will demonstrate the usefulness of the interactive rezoning capabilities and the full thermal/stress calculation for a large strain back extrusion forging.

Thin-wall, back extrusion forgings propose a challenge to both the manufacturer and the computer analyst because the forging process is dominated by large strain, non-isothermal deformation. The fabricator has to overcome problems associated with die chilling, punch heating, and friction to successfully forge this type of component. To accurately model this complex forging process, the FEM deformation code must include heat transfer, contain numerical alogrithms to account for friction between the dies and workpiece, and allow for rezoning as the FEM mesh becomes distorted during simulation of the large strain deformation. Unfortunately, both the manufacturer and analyst are limited by the lack of high temperature (>0.5 T/Tm) and high strain-rate (>10s^{-1}) stress and thermal material property data to assist in their calculations.

The following describes the FEM isothermal and non-isothermal modeling of a two-stage back extrusion forging.

The forging begins as a solid cylinder, 1.94 in. in diameter by 3.35 in. in height which will be forged into a perform configuration for the second-stage, piercing operation. The intentions of the manufacturer was to minimize the number of forging operations thereby lowering the material and labor costs. The dimensions and geometry of the first-stage die and punch are given in Figs. 1a and 1b, respectively. For this particular calculation we modeled the cylinder as an elastic-plastic material (rate and temperature independent) with properties for AF-1410 steel at 900 C. The forging of the preform was modeled as isothermal and did not include the effects of friction. The die and punch were considered elastic materials, therefore non-deformable in the calculation. The loading history was represented by the displacement of the "ram", one inch, approximately 25% of the forging length. The calculation was run in 200 time steps using approximately 15 minutes of CPU time on a Cray-1 and requiring 3 rezoning operations due to the material becoming highly distorted beneath the punch.

The starting mesh and results of the FEM calculation are presented in Figs. 2a, b. The simulation of the preform operation did not indicate any significant problems that would occur during forging. The preform was successfully forged with the manufacturer only noted evidence of small amount of galling on the preform punch.

To evaluate the effect of interface friction on forgeability, the second stage or piercing operation was modeled with and without friction. Again, the die and punch were considered "elastic" materials and the preform given material properties of AF 1410 at 900°C. The dimensions of the punch and die

are illustrated in Fig. 3a and b. The starting mesh for the preform, die and punch shown in Fig. 4a. This same starting geometry was used in all second stage forging calculations. The punch displacement in the second-stage was 3 inches, approximately 75% of the total forging length as shown in Fig. 4b, the final FEM mesh. In the calculation without friction, strains of over 100%, Fig. 5a were concentrated in the forging along the material in contact with the punch. Strains beneath the punch was considerable higher and several rezoning operations were performed in this area.

When a coefficient of 0.2, representing the effect of Coulomb friction was added at the boundaries between the punch, material and die in the next calculation, the strain pattern and magnitude changed. Plastic strains of over 200% formed and were concentrated along the forging and punch interface but additionally along the die and forging interface as shown in Fig. 5b and was not noted in the non-frictional calculation. Friction also increased the values of pressure in the punch which would correspond to a large increase in forming load requirement. If the punch had been modeled as an elastic/plastic material (deformable) large deformations would have occurred. The calculation with friction was made in 245 time steps, required ten rezoning operations and approximately 30 minutes of CRAY 1 CPU time. The addition of friction also required increasing the penalty function at the defined slidelines to avoid penetration. The calculation indicated that the part probably could not be forged in one operation and, if heat transfer were included in the calculation, the likelihood would be decreased even more.

To preform an even more realistic numerical simulation, we included the effects of heat transfer and adiabatic heating due to deformation in the next calculation. This simulation was done with the recently coupled NIKE/TOPAZ 2D FEM code. Due to the lack of thermal data on AF 1410, the billet material was assumed to be 4140 steel and the die and punch material D6 steel. In this calculation the die and punch were modeled as elastic/plastic materials This would allow plastic deformation to occur if the stresses became high enough. Again a friction coefficient of 0.2 was provided for material, at the die and punch interfaces. Properties were provided in NIKE/TOPAZ from handbook sources for Young's modulus, Poisson's ratio, yield strength, tangent modulus, thermal conductivity, heat capacity, density and the coefficient of thermal expansion as a function of temperature (75°F-200°F for 4140 and D6 steels. This calculation was run in 300 time steps at increments of 0.1 simulating a 30 second forging operation. The initial starting temperature of the preform billet was 2000°F and the die and punch were considered to be at ambient temperature (75°F).

The results of the non-isothermal simulation were quite dramatic. The tip of the punch begins rapidly to absorb the heat from the preform forging and rises to above 1700°F within a few seconds into the deformation. The forging immediately begins losing heat to the cooler dies and within seconds, temperatures near the die wall are less than 1000°F. The near instantaneous heating of the punch tip and the cooling of the preform results in a slight upsetting of the punch that begins at approximately 5 seconds into the forming operation. It should be noted that a "gap" exists in the lower region between the preform forging and die wall. The effect of the gap is apparent as no heat transfer is occurring between the forging and die in this area

until the forging comes in contact at these points. By 10 seconds the heat is more evenly distributed in the punch and areas of the forging are shown to be below 600°F. Between 10 and 15 seconds, the forging continues to cool especially in the region around the punch. Temperatures below the punch in the forging and in the tip of the punch drop to less than 1450°F. This will result in the punch effectively increasing in strength. The bulging of the punch has increased the tip diameter effectively increasing the area over which deformation has to occur. At 20 seconds the temperatures have dropped in this region to below 1100°F and the hottest area of the forging, (lower center), is around 1600°F. The punch has actually begun upsetting in the neck region, where there are no physical constraints by the forging. By 25 seconds, the neck of the punch has severly thickened. This trend continues and by 30 seconds the punch is quite deformed, shows two distinct bulged regions, and core temperatures in the forging are below 1400°F. This sequence is illustrated in a series of ORION plots, where Figs. 6a-d show the deformed mesh at 5, 10, 20 and 30 seconds. Figs. 7a-e, show the temperature/deformation history at 0, 5, 10, 20, 30 seconds and Fig. 8 shows effective plastic strain at 30 seconds in final forging.

The two phases of deformation can be easily explained in the following manner. The initial bulging of the punch is directly associated with rapid high temperature heat transfer and subsequent lowering of mechanical properties that allows the punch to upset at the tip. As the forging process continues, cooling dominates and the preform and punch begin to have resistance to flow. The second bulge occurs as high unrestrained stresses develop in the neck. Therefore, at first, heat transfer dominates the process, and the punch material is limited by high temperature strength, whereas, secondly, in the subsequent bulging in the neck region, the punch material is limited purely by yield strength.

To "test" this theory an additional analysis was performed with all of the same conditions except that the strength of the punch material was not temperature dependent, that is, heating was not allowed to lower the yield strength. This reflects the vendors suggestion that the problem might be eliminated by a punch made from material with higher hot strength. In this analysis the punch does severely deform but in a manner quite different from the previous calculation. The first obvious difference is that although the heat transfer is occurring into the punch, no bulging of the tip is evident. At 15 seconds, the punch begins to deform but in the region just past the top edge of the forging where temperatures are still quite low. This trend of severe upsetting continues throughout the 30-second forging operation and finally a well-defined bulge is formed, where Figs. 9a-d show deformed mesh at 5, 10, 20 and 30 seconds. Figs. 10a-d the temperature/deformation history at 5, 10, 20 and 30 seconds and Fig. 11 the effective plastic strain at 30 seconds in final forging.

Each of these calculations took roughly 20 minutes of CPU time on a CRAY1 and required several rezoning operations. Full coupling of NIKE2D and TOPAZ2D did not add to the amount of CPU time required for the calculation.

The actual forging of the second stage was never successfully completed. The punch did indeed upset destroying the tooling. Several suggestions were made to remedy the situation: intermediate stage tooling, reheating of forging and possibly using faster forming equipment such as the DYNAPAK. Unfortunately, additional funds are not available to explore these possibilities.

On the positive side, calculations, such as these, demonstrate that one can effectively <u>watch</u> the effects of heat flow and deformation simultaneously during a forming operation. It can be assured that this visualization process holds great promise in further understanding metal deformation behavior during forming of complex geometry components. A large strain, two-stage back extrusion forging has been analyzed both isothermally with and without friction, and non-isothermally with friction for two different punch materials. Interactive rezoning was a necessary feature of the FEM code to obtain a solution. In the isothermal analysis, friction was shown to effect the strain distribution in the forging and contribute to high stresses in the punch. Full coupling of the NIKE2D stress analysis FEM code with TOPAZ2D heat transfer FEM code provided the capability for non-isothermal analyses. The results of the analyses were quite dramatic in showing the combined effects of heat transfer and deformation on the final part geometry and the distribution of stresses and strains. Full solution calculations that account for both large strain deformation and heat transfer show great promise in further understanding the deformation behavior of metals during complex metal forming operations.

ACKNOWLEDGMENTS

References

1. J. O. Hallquist, <u>NIKE2D--A Vectorized, Implicit, Finite Deformation,</u> <u>Finite-Element Code for Analyzing the Static and Dynamic Response of 2-D</u> <u>Solids,</u> Lawrence Livermore National Laboratory, Livermore, CA, UCRL-19677 (1983).

2. E. C. Flower and J. O. Hallquist, <u>Computer-Aided Simulation of Metal</u> <u>Forming,</u> Lawrence Livermore National Laboratory, Livermore, CA UCRL-93634 (1986)

3. A. B. Shapiro <u>TOPAZ--A Finite Element Heat Conduction Code for Analyzing</u> <u>2-D Solids,</u> Lawrence Livermore National Laboratory, Livermore, CA, UCID-20045 (1986).

4. A. B. Shapiro and K. W. Mahin, <u>Thermal Mechanical Modeling of Gas</u> <u>Tungsten Arc Welding,</u> Lawrence Livermore National Laboratory, Livermore, CA, UCRL-94627.

5. Ron Wallis, Cameron Iron Works, Inc., Houston, Texas, private communication.

6. J. O. Hallquist, <u>MAZE--An Input Generator for DYNA2D and NIKE2D,</u> Lawrence Livermore National Laboratory, Livermore, CA, UCRL-19029, Rev. 2 (1983).

7. J. O. Hallquist and J. L. Levatin, <u>ORION: An Interactive Color</u> <u>Post-processor for Two-Dimensional Finite-Element Codes,</u> Lawrence Livermore National Laboratory, Livermore, CA, UCRL-19310, Rev. 2 (1985).

Figure Captions

Fig. 1.   Dimension of a) preform punch
                        b) preform die

Fig. 2.   FEM Mesh Preform - die, punch
                        a) billet - before deformation
                        b) forging - after deformation

Fig. 3.   Dimensions of Second-Stage
                        a) punch
                        b) die

Fig. 4.   FEM Mesh - forging, die, punch
                        a) Before deformation
                        b) After deformation

Fig. 5.   Effective plastic strains in final forging
                        a) Isothermal - no friction
                        b) Isothermal - with friction

Figs. 6a-d   FEM Mesh (5 sec - 30 sec)
               Temperature Dependent Punch

Figs. 7a-e   Contour Plots Temperature/Deformation (0 sec - 30 sec)
               Temperature Dependent Punch

Fig. 8   Effective Plastic Strain (30 sec)
         Temperature Dependent Punch

Figs. 9a-d   FEM Mesh (5 sec - 30 sec)
               Non-Temperature Dependent Punch

Fig. 10a-d   Contour Plots of Temperature/Deformation (5 sec - 30 sec)
               Non-Temperature Dependent Punch

Fig. 11 Effective Plastic Strain (30 sec)
         Non-Temperature Dependent Punch

0743G

1°

3.413

1.016

0.254 SR

1.940 diam.

(a) 1st-stage punch

1.970 diam.

1°

3.413

3.961

3.148 SR

(b) 1st-stage die

1.463 diam.
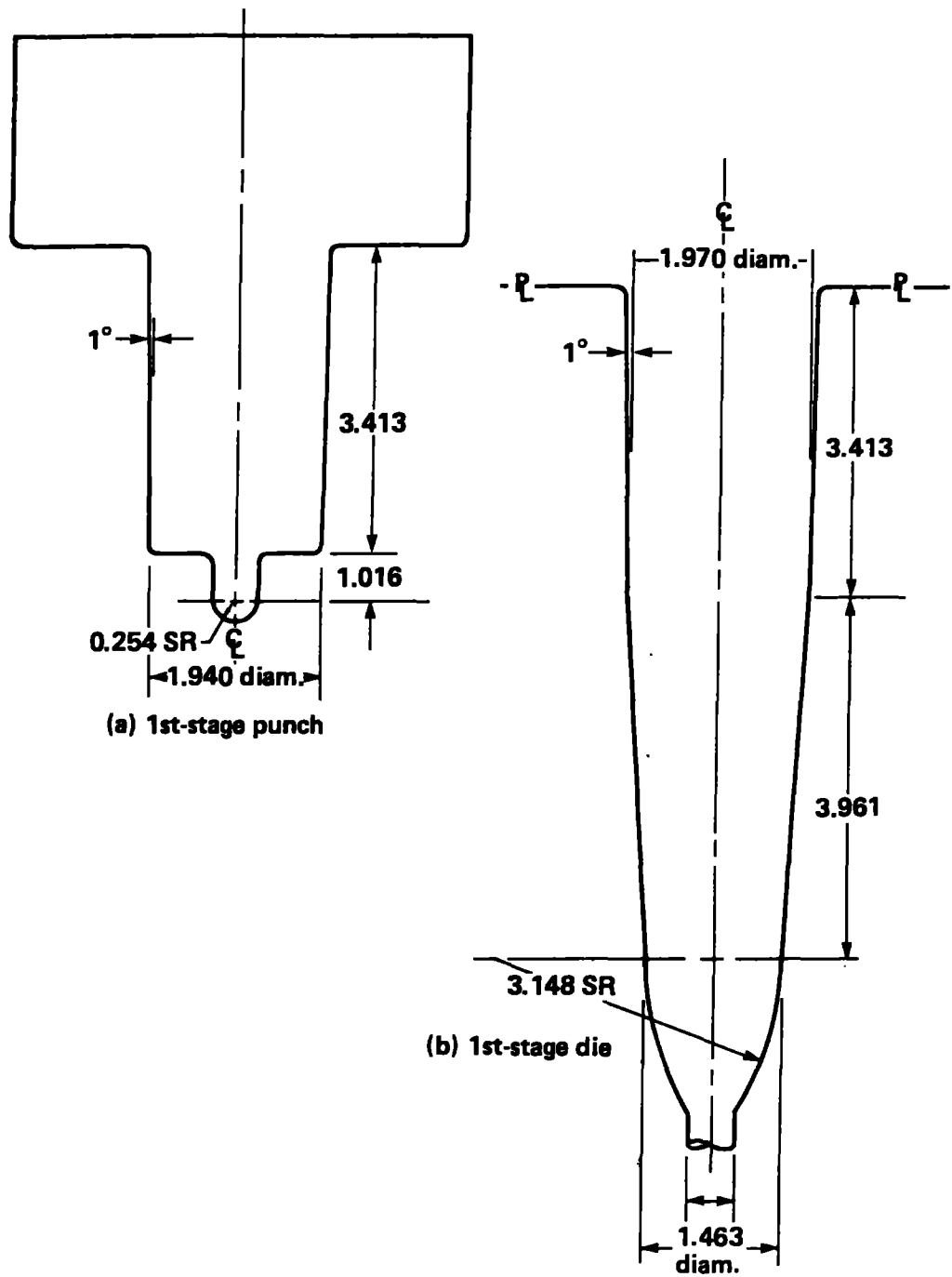
Fig. 1
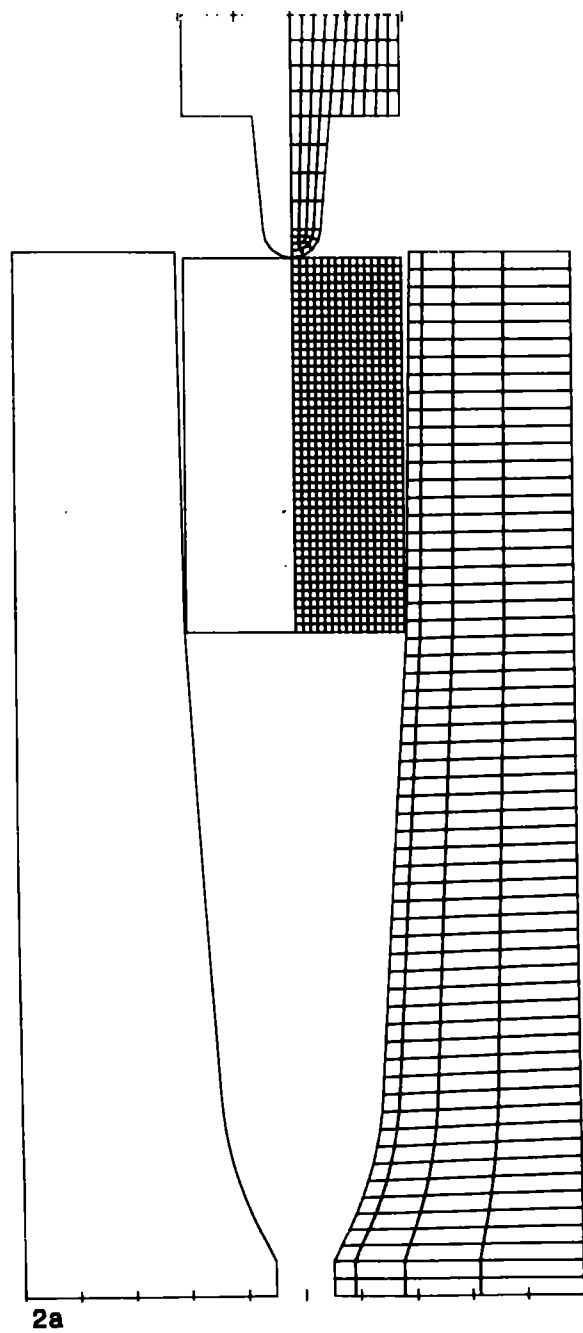
Preform – Isothermal without Friction

Fig. 2

2a

2b

2.00 Ref.

0.763

1°

1.244 diam.

4.951

0.254

Ⴚ

(a) 2nd-stage punch

2.031 diam.

Ⴑ

3.174 SR

(b) 2nd-stage die

Vent hole

1.523 diam.
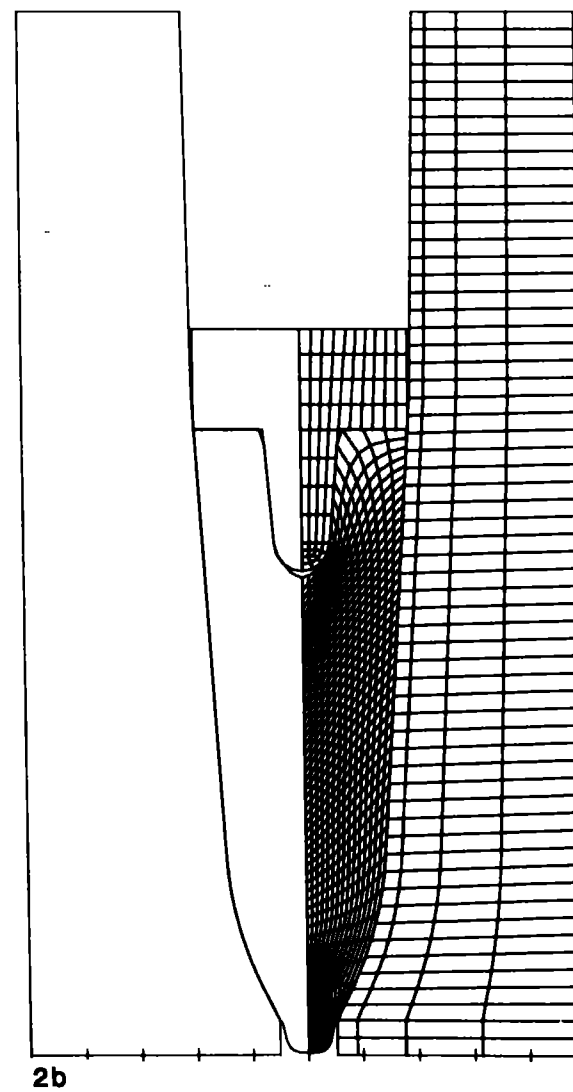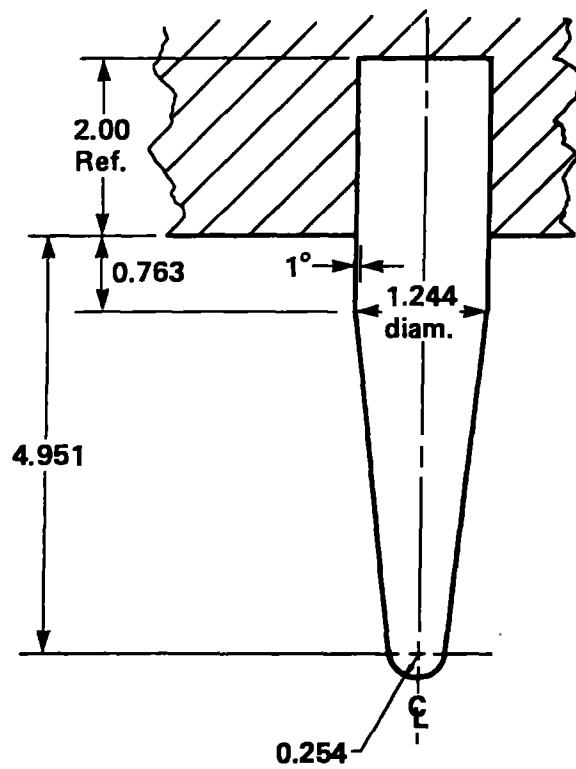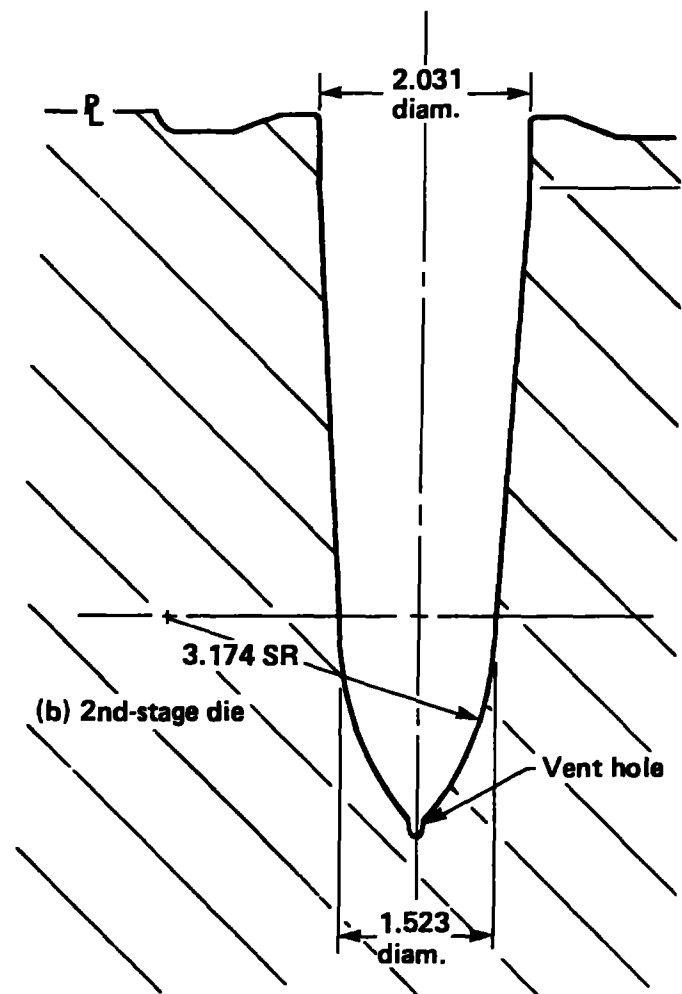
Fig. 3
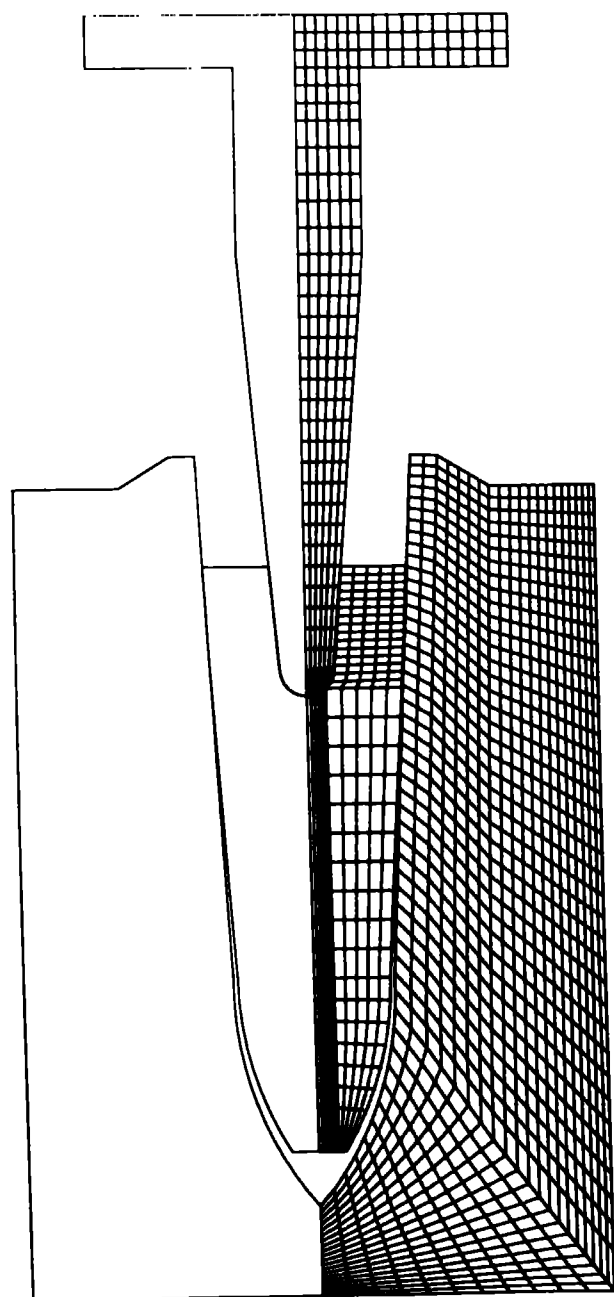
Second Stage

Isothermal

Fig. 4

4a

4b

min(-)= 0.
max(+)= 1.57e+01

contour levels
a= 1.57e+00
b= 3.14e+00
c= 4.71e+00
d= 6.28e+00
e= 7.85e+00
f= 9.43e+00
g= 1.10e+01
h= 1.26e+01
i= 1.41e+01

min(-)= 0.
max(+)= 1.2℃

contour le
a= 1.75
b= 3.51
c= 5.26
d= 7.02
e= 8.77
f= 1.05

5a

5b
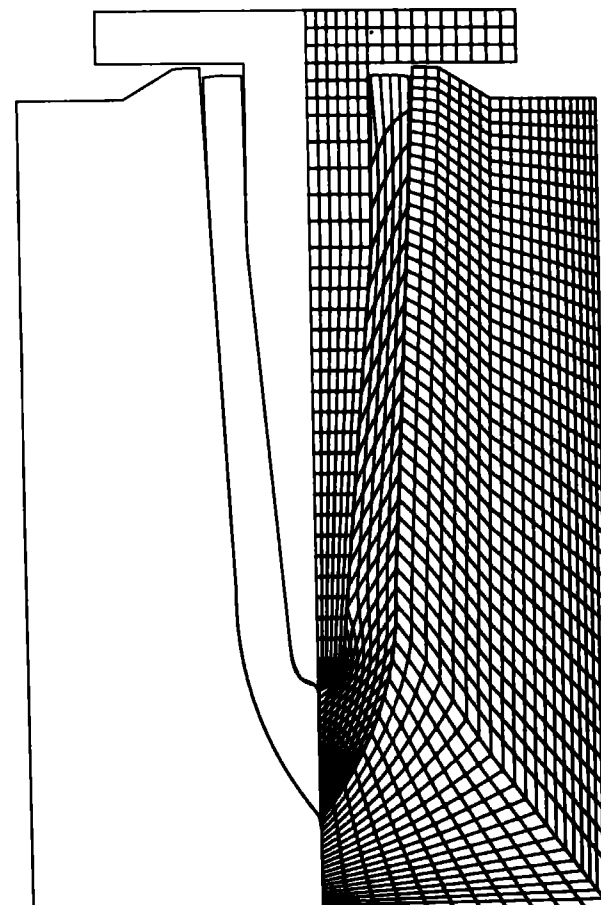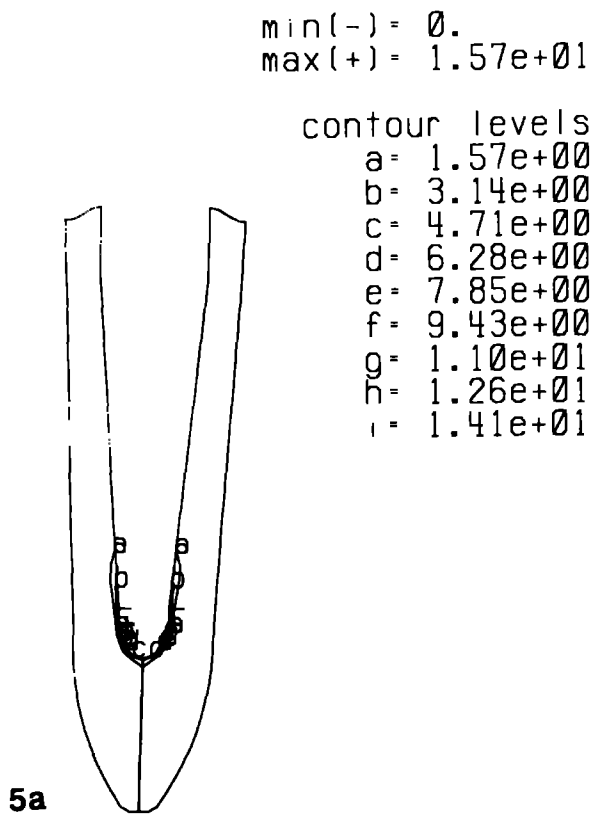
Isothermal without Friction
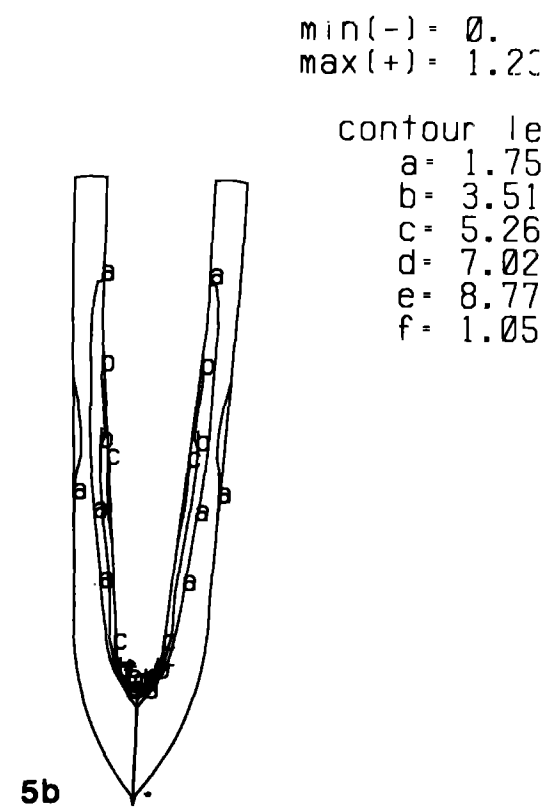
Isothermal with Friction

Fig. 5

Second Stage - Non-Isothermal with Friction - A
      time=   5.00000e+00
      dsf =   1.00000e+00

6a   5 sec
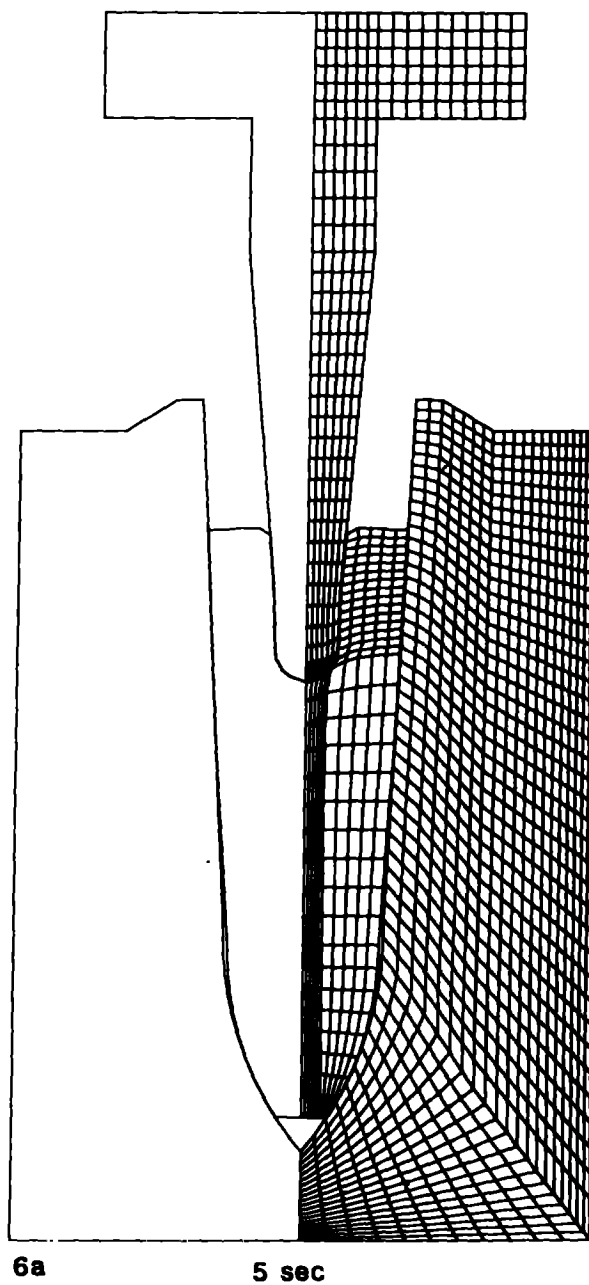
Fig. 6(a)

Second Stage - Non-Isothermal with Friction   A
        time =   1.00000e+01
        dsf =   1.00000e+00
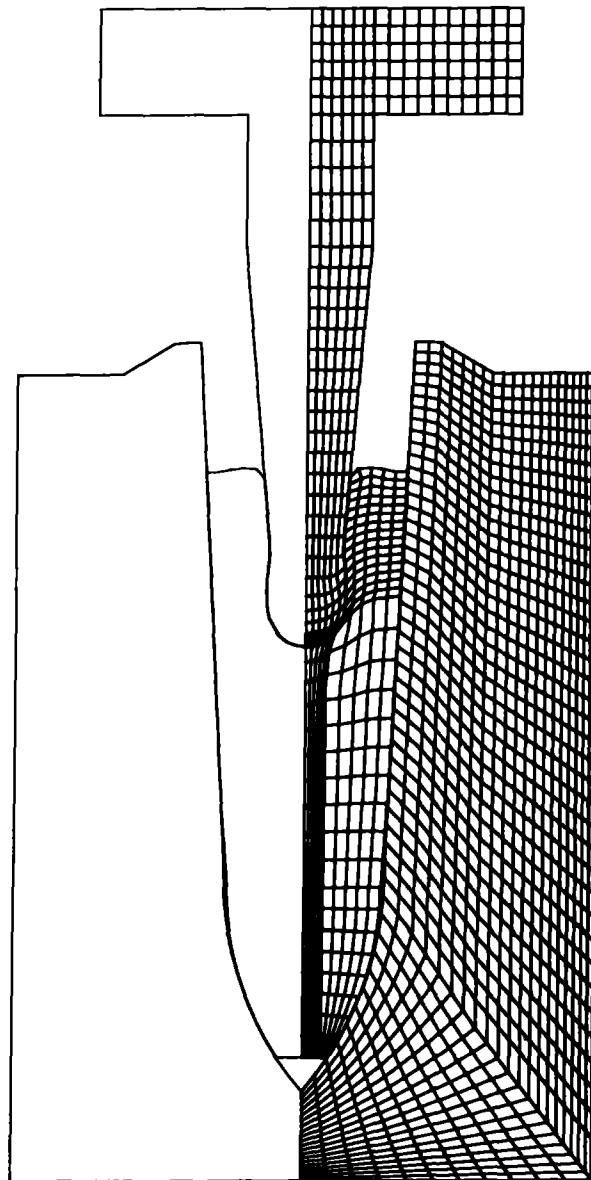
6b

10 sec

Fig. 6(b)

Second Stage - Non-Isothermal with Friction - A
time: 2.00000e+01
dsf : 1.00000e+00
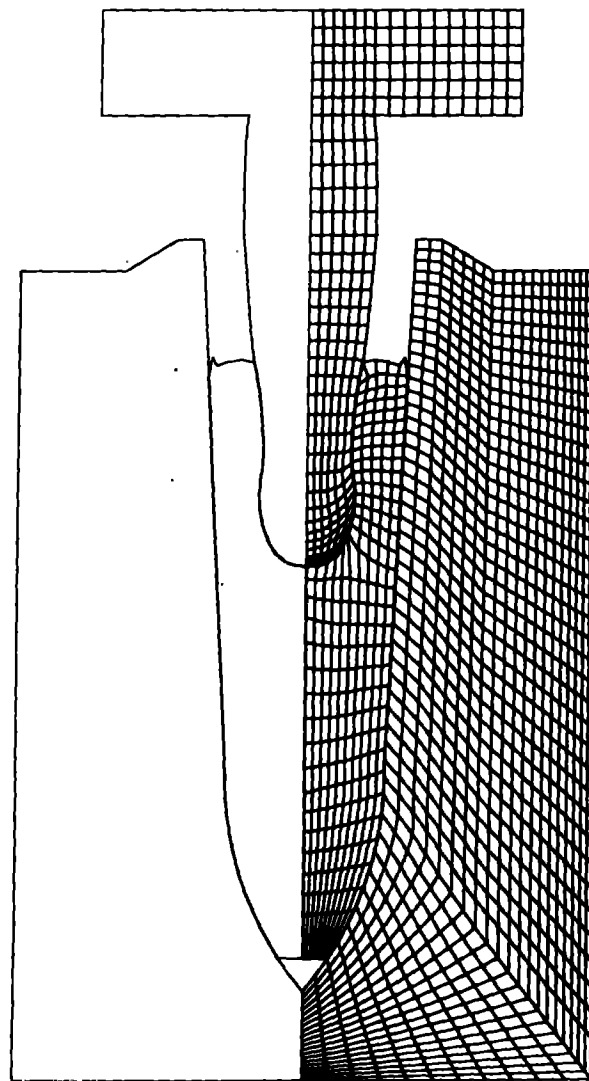
6c

20 sec

Fig. 6(c)

Second Stage - Non-Isothermal with Friction - A
         time=   3.00000e+01
         dsf =   1.00000e+00
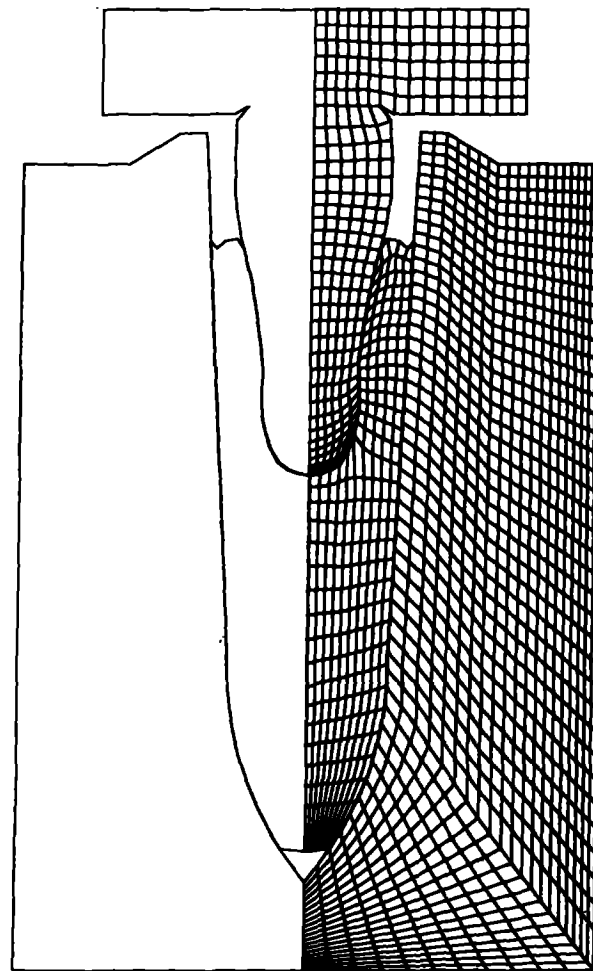
6d

30 sec

Fig. 6(d)

Second Stage - Non-Isothermal with Friction - A
    time=   0.
    dsf =   1.00000e+00 contours of temperature
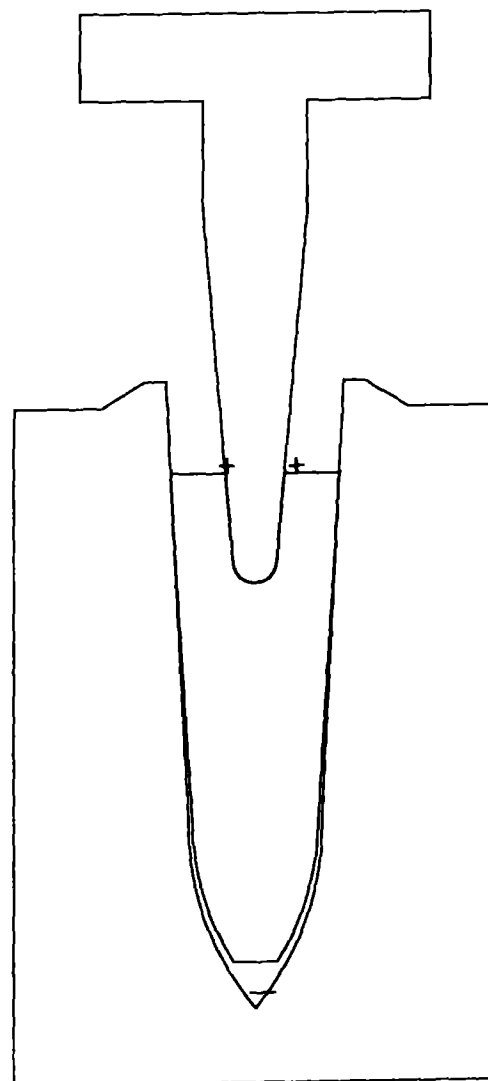
min(-)= 7.50e+01
max(+)= 2.00e+03

contour levels
    a= 3.50e+02
    b= 6.25e+02
    c= 9.00e+02
    d= 1.17e+03
    e= 1.45e+03
    f= 1.72e+03

7a

0 sec

Fig. 7(a)

Second Stage - Non-Isothermal with Friction - A
time= 5.00000e+00
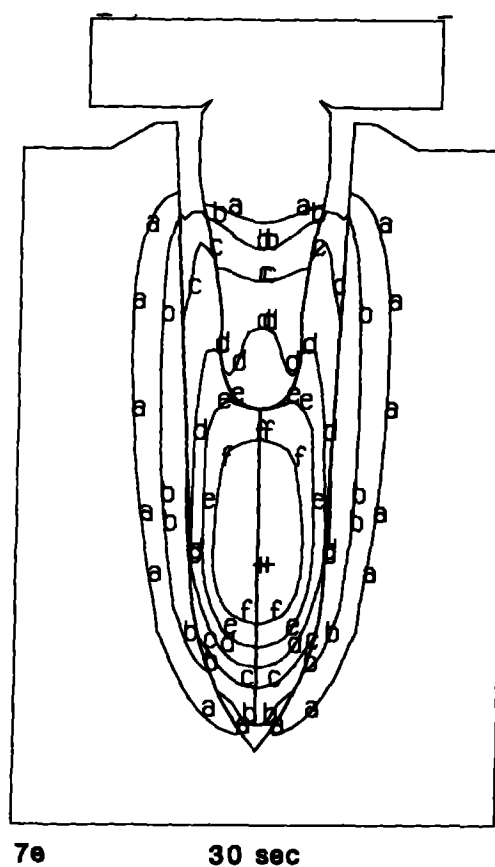dsf = 1.00000e+00 contours of temperature

min(-)= 7.50e+01
max(+)= 2.00e+03

contour levels
a= 3.50e+02
b= 6.25e+02
c= 9.00e+02
d= 1.17e+03
e= 1.45e+03
f= 1.72e+03

7b   5 sec
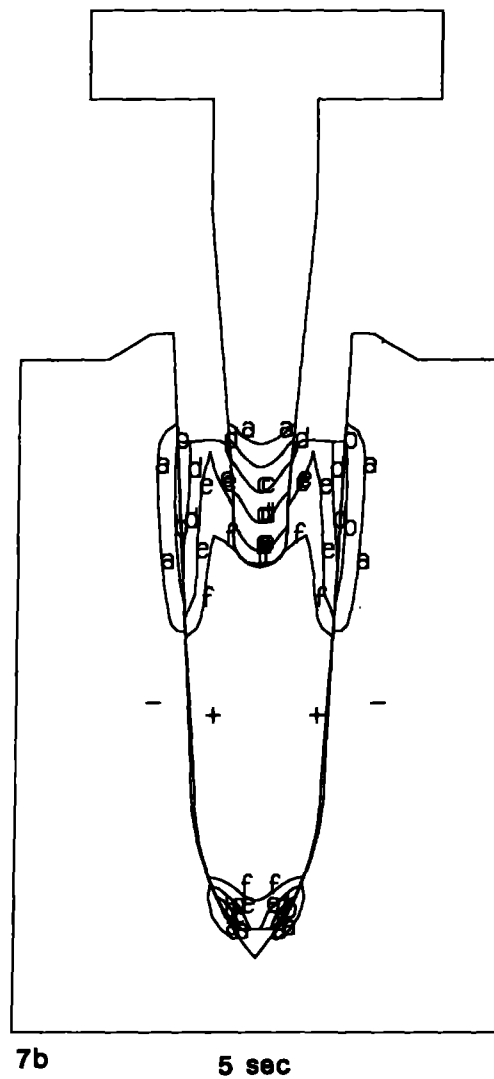
Fig. 7(b)

Second Stage – Non-Isothermal with Friction – A
time = 1.00000e+01
dsf = 1.00000e+00 contours of temperature

min(-) = 7.50e+01
max(+) = 2.00e+03

contour levels
a = 3.50e+02
b = 6.25e+02
c = 9.00e+02
d = 1.17e+03
e = 1.45e+03
f = 1.72e+03

7c   10 sec
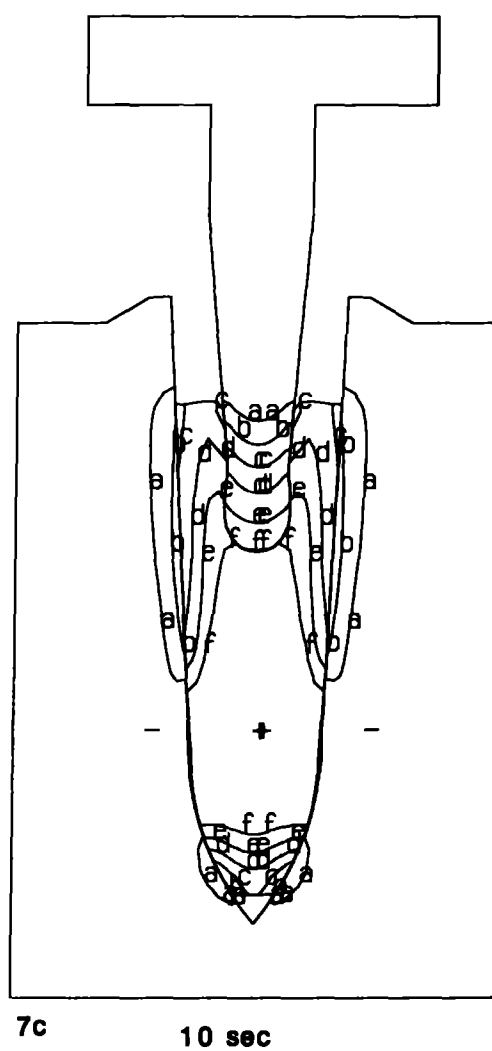
Fig. 7(c)

Second Stage - Non-Isothermal with Friction - A
time= 2.00000e+01
dsf = 1.00000e+00 contours of temperature
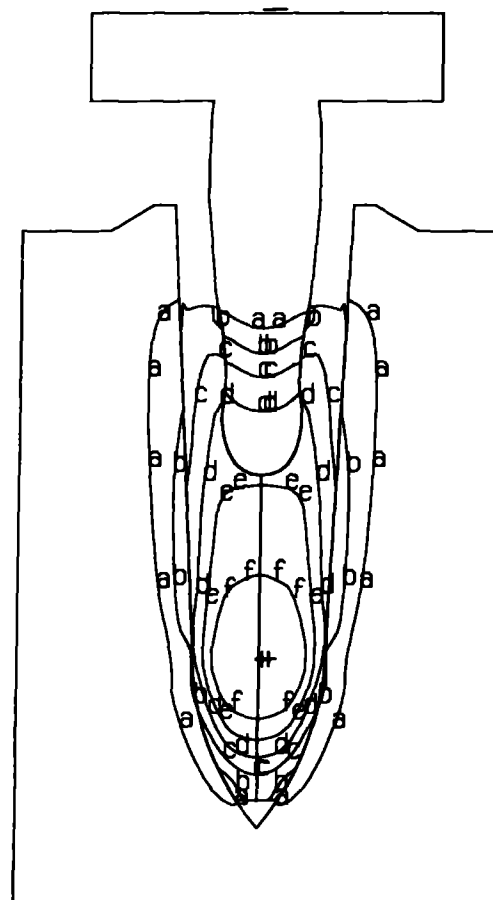
min(-)= 7.50e+01
max(+)= 1.87e+03

contour levels
a= 3.32e+02
b= 5.89e+02
c= 8.46e+02
d= 1.10e+03
e= 1.36e+03
f= 1.62e+03

7d   20 sec

Fig. 7(d)

Second Stage - Non-Isothermal with Friction - A
time = 3.00000e+01
dsf = 1.00000e+00 contours of temperature

min(-) = 7.50e+01
max(+) = 1.38e+03

contour levels
a = 2.62e+02
b = 4.49e+02
c = 6.36e+02
d = 8.23e+02
e = 1.01e+03
f = 1.20e+03

7e   30 sec

Fig. 7(e)

Second Stage - Non-Isothermal with Friction - A
time= 3.00000e+01
dsf = 1.00000e+00 contours of effective plastic str
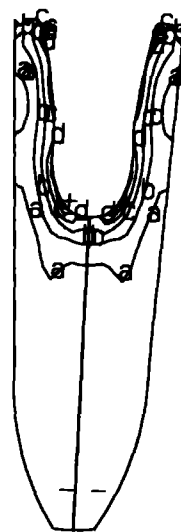
min(-) = 1.07e-02
max(+) = 1.62e+00

contour levels
a= 2.41e-01
b= 4.71e-01
c= 7.01e-01
d= 9.31e-01
e= 1.16e+00
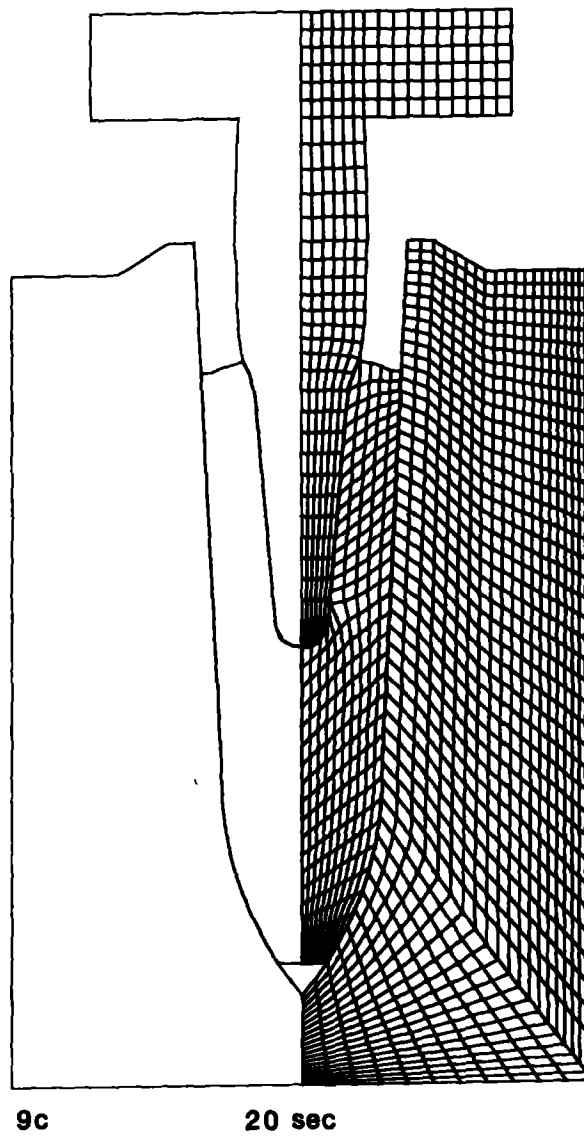f= 1.39e+00

Time = 30 sec

Fig. 8

Second Stage - Non-Isothermal with Friction - J
        time=   5.00000e+00
        dsf =   1.00000e+00
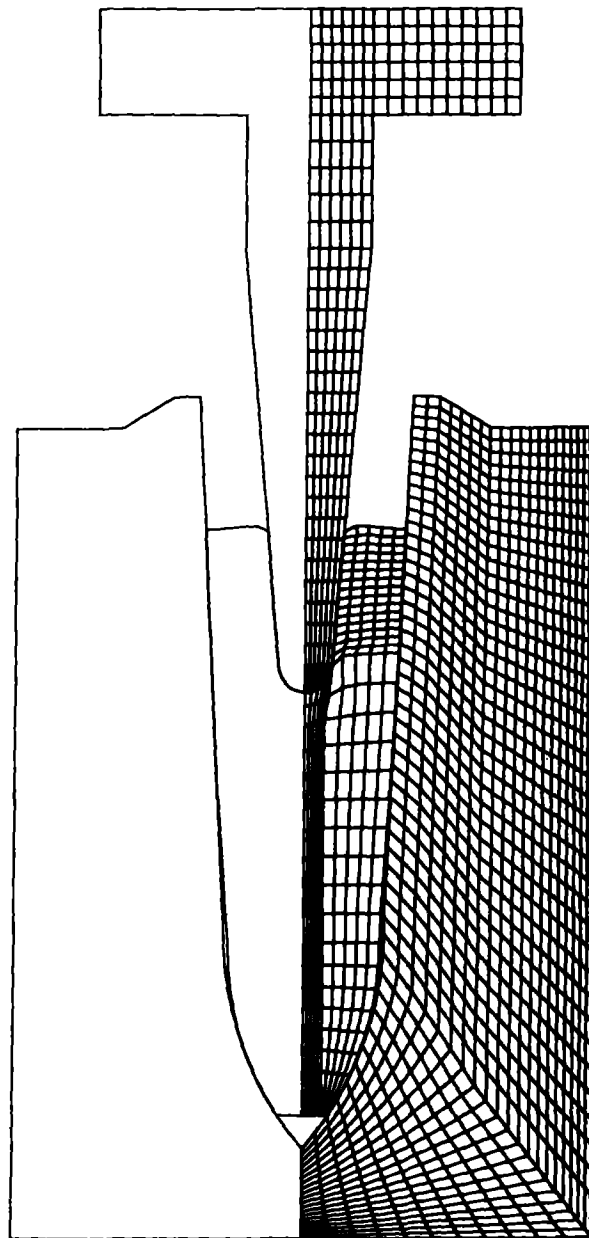
9a

5 sec

Fig. 9(a)

Second Stage - Non-Isothermal with Friction - J
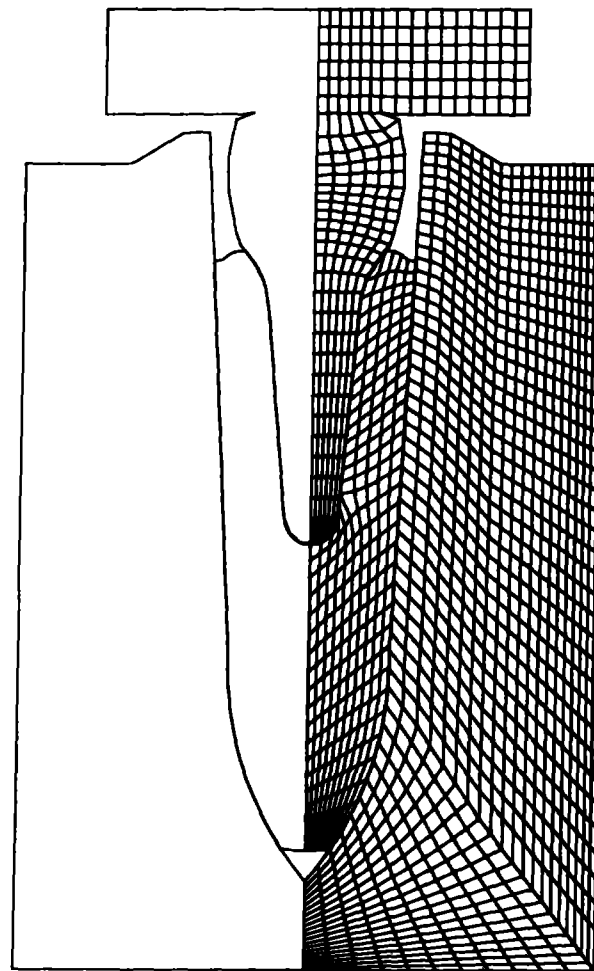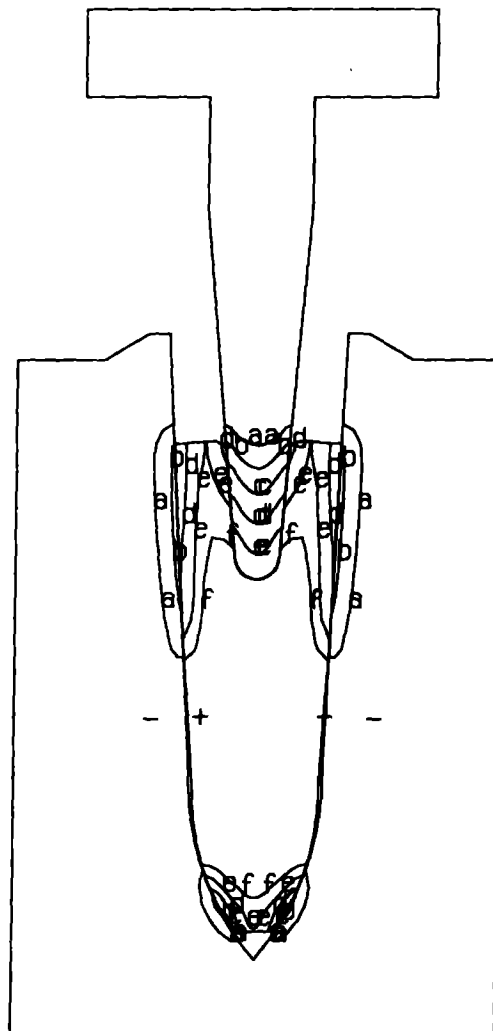time= 1.00000e+01
dsf = 1.00000e+00

9b

10 sec

Fig. 9(b)

9c   20 sec

Fig. 9(c)

9d

30 sec

Fig. 9(d)

Second Stage - Non-Isothermal with Friction - J
  time=   5.00000e+00
  dsf =   1.00000e+00 contours of temperature

min(-) = 7.50e+01
max(+) = 2.00e+03

contour levels
  a= 3.50e+02
  b= 6.25e+02
  c= 9.00e+02
  d= 1.17e+03
  e= 1.45e+03
  f= 1.72e+03

10a   **5 sec**

Fig. 10(a)

Second Stage - Non-Isothermal with Friction - J
time = 1.00000e+01
dsf = 1.00000e+00 contours of temperature

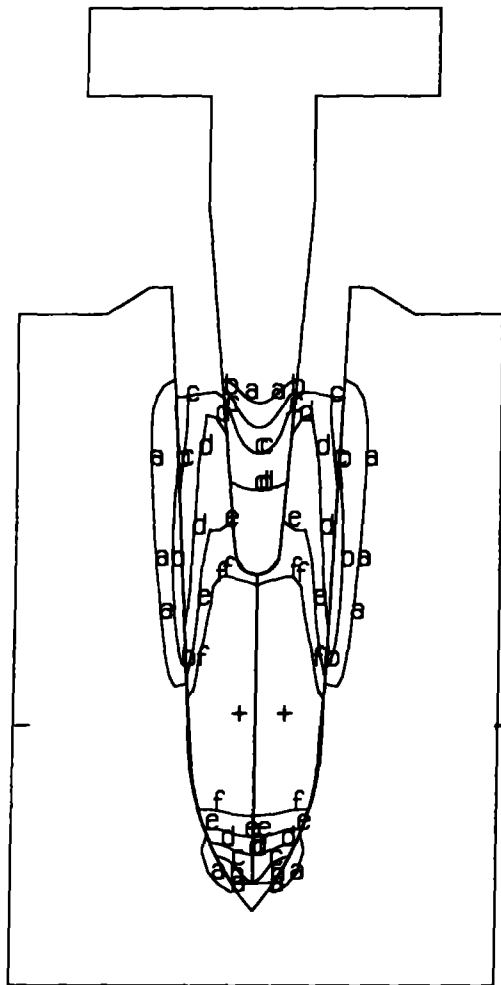min(-) = 7.50e+01
max(+) = 2.00e+03

contour levels
a = 3.50e+02
b = 6.25e+02
c = 9.00e+02
d = 1.17e+03
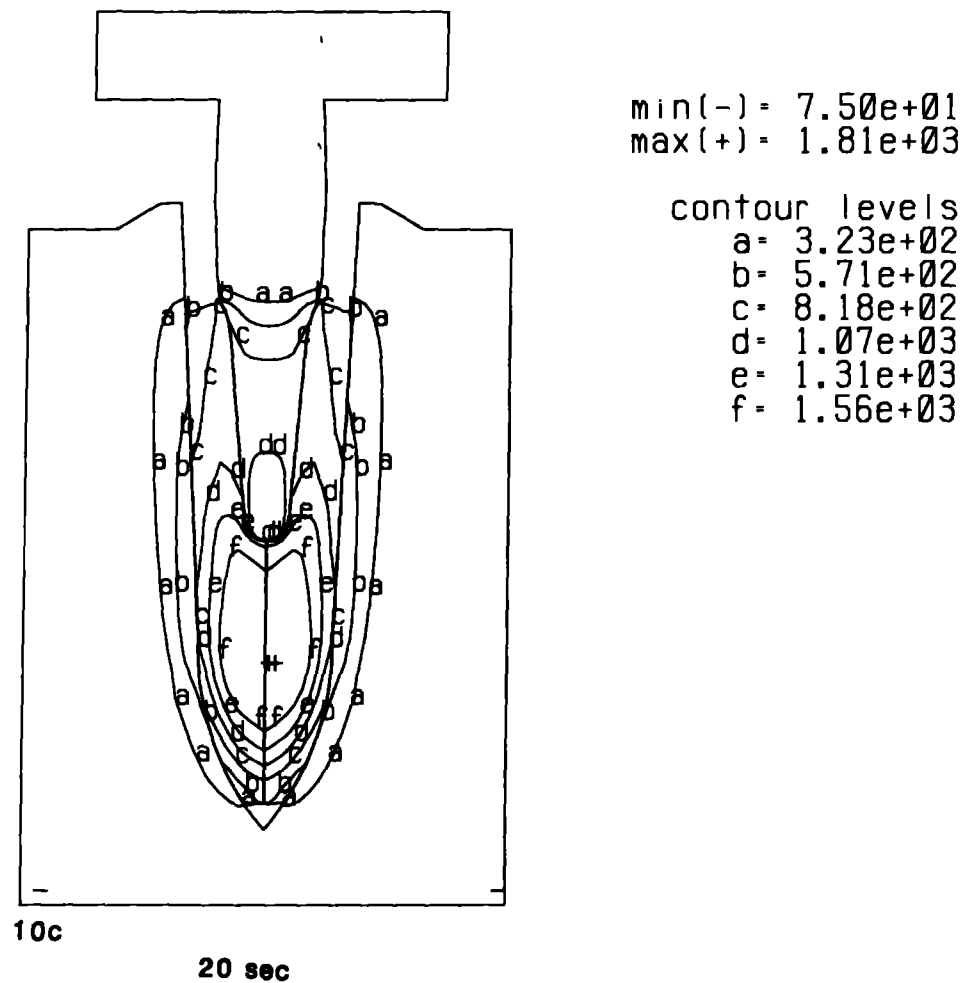e = 1.45e+03
f = 1.72e+03

10b   **10 sec**

Fig. 10(b)

Second Stage - Non-Isothermal with Friction - J
time = 2.00000e+01
dsf = 1.00000e+00 contours of temperature

min(-) = 7.50e+01
max(+) = 1.81e+03

contour levels
a = 3.23e+02
b = 5.71e+02
c = 8.18e+02
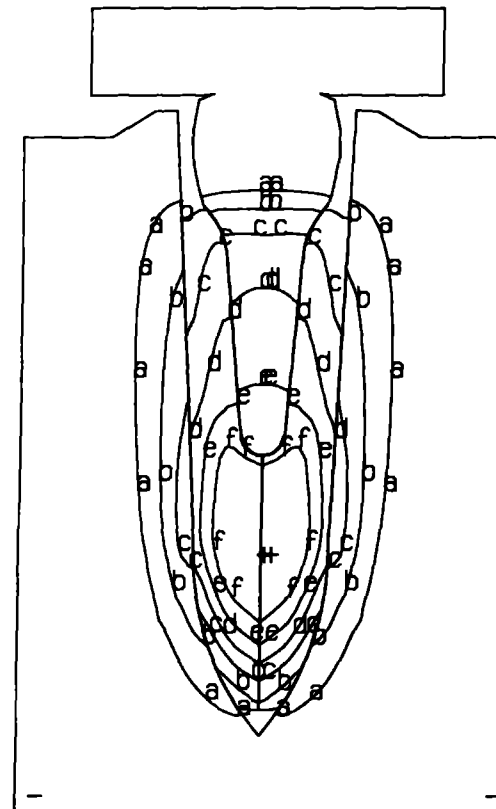d = 1.07e+03
e = 1.31e+03
f = 1.56e+03

10c

20 sec

Fig. 10(c)

Second Stage - Non-Isothermal with Friction - J
time=   3.00000e+01
dsf =   1.00000e+00 contours of temperature

min(-) = 7.50e+01
max(+) = 1.40e+03

contour levels
   a = 2.64e+02
   b = 4.54e+02
   c = 6.43e+02
   d = 8.32e+02
   e = 1.02e+03
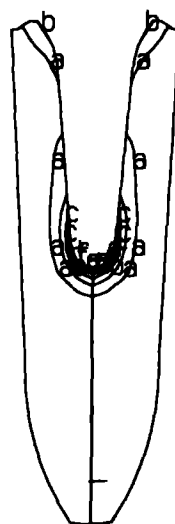   f = 1.21e+03

10d   **30 sec**

Fig. 10(d)

Second Stage - Non-Isothermal with Friction - J
time = 3.00000e+01
dsf = 1.00000e+00 contours of effective plastic strain

min(-) = 1.96e-02
max(+) = 3.05e+00

contour levels
a = 4.53e-01
b = 8.86e-01
c = 1.32e+00
d = 1.75e+00
e = 2.19e+00
f = 2.62e+00

Time = 30 sec

Fig. 11